tiate between the complexation behaviors of MIDA and IDA.

Conclusions

The *relative* intensities observed among the $^7F_J \leftarrow {}^5D_0$ transitions in the unpolarized emission spectra reported in this study demonstrate the "hypersensitivity" of the $^7F_2 \leftarrow {}^5D_0$ transition to the ligand environment. Relative to the $^7F_1 \leftarrow {}^5D_0$ transition, this transition is most intense for the 1:3 Eu^{3+}/DPA system and least intense for $EuCl_3$ in water. This result supports the prediction of the ligand polarization model for hypersensitivity,[21,22] which states that the intensity of a hypersensitive transition should correlate with the dipolar polarizability of the ligand environment. Among the ligands examined in this study, DPA contains the most polarizabile group (the pyridyl moiety) while H_2O is the least polarizable.

The nearly identical unpolarized emission spectra obtained for microcrystalline $Na_3[Eu(ODA)_3]\cdot 2NaClO_4\cdot 6H_2O$ and 1:3 Eu^{3+}/ODA in aqueous solution suggest that the dominant species in solution is $Eu(ODA)_3^{3-}$, a tris-terdentate complex having trigonal dihedral (D_3) symmetry. The $^7F_{1,2} \leftarrow {}^5D_0$ MCPL spectra observed for the 1:3 Eu^{3+}/ODA solution samples are entirely compatible with such a structure. In fact, these spectra provide a near "textbook" example of what one expects for an axially symmetric Eu(III) complex in which the $h^+(2,0)$ component of the crystal field is relatively weak. The MCPL/emission spectra observed for the 1:3 Eu^{3+}/DPA system also conform exactly to that predicted for complexes of trigonal dihedral (D_3) symmetry. In this case, however, the $^7F_1 \leftarrow {}^5D_0$ MCPL/emission results reveal a relatively strong $h^+(2,0)$ crystal field component. The MCPL spectra obtained for the 1:5 Eu^{3+}/MIDA solution samples are identical with those predicted for a complex having C_{3h} symmetry, and the absence of any observed splitting within the $^7F_1 \leftarrow {}^5D_0$ transition region in the unpolarized spectra suggests a relatively weak $h^+(2,0)$ crystal field component. These results indicate that tris-terdentate $Eu(MIDA)_3^{3-}$ complexes of C_{3h} symmetry are the dominant species present in the 1:5 Eu^{3+}/MIDA solution samples.

Among the systems investigated in this study, only 1:5 Eu^{3+}/IDA in aqueous solution gave MCPL results suggesting the dominance of nonaxially symmetric structures. Given the $[Eu^{3+}]$:[IDA] concentration ratio (1:5) and pH conditions used in this study, it is likely that the dominant coordination species is $Eu(IDA)_3^{3-}$. However, in this case each bound IDA ligand possesses a >N-H group that is capable of promoting outer-sphere coordination to excess (unbound) ligands in solution. Since these outer-sphere complexes would be expected, in general, to possess nonaxially symmetric structures, it may be postulated that they account for the observed MCPL behavior of the 1:5 Eu^{3+}/IDA system.

It is clear that MCPL spectra can provide structural information not readily obtainable by the use of other techniques. Most previous applications of MCPL have been in studies of ions in crystals at low temperatures.[25-28] However, the results reported here demonstrate that it can also be used to great advantage in the study of lanthanide complexes in solution media at room temperature.

Acknowledgment. This work was supported by the National Science Foundation (NSF Grant CHE80-04209).

Registry No. $(ODA)_3^{3-}$, 43030-81-5; $Eu(DPA)_3^{3-}$, 38721-36-7; $Eu(IDA)_3^{3-}$, 87727-55-7; $Eu(MIDA)_3^{3-}$, 87682-22-2; $EuCl_3$, 10025-76-0.

(25) Morley, J. P.; Faulkner, T. R.; Richardson, F. S. *J. Chem. Phys.* **1982**, *77*, 1710.
(26) Morley, J. P.; Faulkner, T. R.; Richardson, F. S.; Schwartz, R. W. *J. Chem. Phys.* **1982**, *77*, 1734.
(27) Schwartz, R. W.; Brittain, H. G.; Riehl, J. P.; Yeakel, W.; Richardson, F. S. *Mol. Phys.* **1977**, *34*, 361.
(28) Luk, C. K.; Yeakel, W. C.; Richardson, F. S. *Chem. Phys. Lett.* **1975**, *34*, 147.

Contribution from the Departments of Chemistry, University of Virginia, Charlottesville, Virginia 22901, and Virginia Commonwealth University, Richmond, Virginia 23298

Magnetic Circularly Polarized Luminescence Spectra of Eu(β-diketonate)$_3$X$_2$ Complexes in Nonaqueous Solution

DAVID R. FOSTER,† F. S. RICHARDSON,*† L. M. VALLARINO,‡ and DONALD SHILLADY‡

Received January 14, 1983

Unpolarized emission spectra and magnetic field induced circularly polarized emission spectra are reported for $EuCl_3$ and for five different tris(β-diketonate) Eu(III) complexes in methanol and in *N*,*N*-dimethylformamide solutions. Analysis of the $EuCl_3$ spectra suggests the predominance of *axially* symmetric coordination species with C_{3v} point-group symmetry. Analysis of the tris(β-diketonate) Eu(III) spectra show the predominance of *nonaxially* symmetric structures with very strong orthorhombic crystal field components. The observed $^7F_2 \leftarrow {}^5D_0$ and $^7F_1 \leftarrow {}^5D_0$ emission intensity ratios exhibit a strong sensitivity to the structural details and chemical nature of the ligand environment, with the magnitude of $I(^7F_2 \leftarrow {}^5D_0)$:$I(^7F_1 \leftarrow {}^5D_0)$ correlating closely with ligand or ligand substituent polarizabilities. The latter is explained in terms of the ligand dipolar polarization model for 4f → 4f electric dipole intensities. The $^7F_0 \leftarrow {}^5D_0$ transition intensity (relative to that of $^7F_1 \leftarrow {}^5D_0$) is also observed to be very sensitive to the ligand environment, and this is attributed to its "stealing" intensity from the $^7F_2 \leftarrow {}^5D_0$ transition via a mechanism involving crystal field induced mixings between the $^7F_0$ and $^7F_2$ (and $^5D_0$ and $^5D_2$) multiplet states.

Introduction

In the preceding paper,[1] we reported magnetic circularly polarized luminescence (MCPL) spectra obtained on four different Eu^{3+}–ligand systems that, in aqueous solution under basic conditions, were shown to form predominantly tris-terdentate (9-coordinate) complexes with trigonal symmetry (either D_3 or C_{3h}). In the present paper, we report MCPL spectra for a series of 8-coordinate Eu(β-diketonate)$_3$X$_2$ complexes dissolved in either methanol (MeOH) or *N*,*N*-dimethylformamide (DMF). In this series, the β-diketonate ligands differ with respect to their substituent groups and X represents either a water molecule or a solvent molecule

† University of Virginia.
‡ Virginia Commonwealth University.

(1) Foster, D.; Richardson, F. S. *Inorg. Chem.*, preceding paper in this issue.

0020-1669/83/1322-4002$01.50/0

(MeOH or DMF). An MCPL spectrum is also reported for an 8-coordinate Eu(β-diketonate)$_3$(*o*-phen) complex, where *o*-phen = 1,10-phenanthroline (or *o*-phenanthroline). Unlike the complexes examined in ref 1, which had axially symmetric (or *nearly* axially symmetric) structures, the complexes examined in this study are predicted to have nonaxially symmetric structures with either C_2 or C_s "effective" symmetry.[2] This prediction is predicated, in part, on the assumption that 8-fold coordination is retained in solution, with the X ligands occupying two specific coordination sites.

One of the possible alternatives to the predominance of nonaxially symmetric 8-coordinate structures for the systems investigated here in solution media is the dominant existence of "effectively" 6-coordinate Eu(β-diketonate)$_3$ complexes that, on average, may have axially symmetric structures. In fact, in the use of Ln(β-diketonate)$_3$ complexes as NMR shift reagents,[3] it has often been assumed that the Ln(β-diketonate)$_3$S adduct species (where S denotes an organic substrate molecule whose NMR spectrum is being measured) are axially symmetric. This, of course, implies an axially symmetric Ln(β-diketonate)$_3$ structure. Although the correctness of this assumption has been called into question by Horrocks and co-workers,[4-6] it continues to be used in the interpretation of NMR data obtained for organic molecules bound as substrates to Ln(β-diketonate)$_3$ shift reagents in solution. Europium(III) $^7F_{0,1,2} \leftarrow {}^5D_0$ MCPL provides an excellent probe for differentiating between axially symmetric and nonaxially symmetric structures of Eu(III) complexes. This application of Eu(III) MCPL was discussed in the preceding paper,[1] and it has already been employed in structural studies of several Eu(β-diketonate)$_3$ complexes in DMF and Me_2SO (dimethyl sulfoxide) solutions.[7] Four different Eu(β-diketonate)$_3$ systems were included in the latter studies,[7] and in each case the MCPL results demonstrated the predominance of nonaxially symmetric structures. Furthermore, detailed analysis of the $^7F_1 \leftarrow {}^5D_0$ MCPL spectra led to estimates for the magnitudes of the lowest order, nonaxially symmetric, even-parity crystal field coefficients for each of the systems.

The main objectives of the present study are similar to those that motivated the studies reported in ref 7. However, in the present study, closer attention is paid to possible solvent effects and to ligand substituent effects. Of special interest in the latter regard are differential crystal field effects exerted by symmetrically substituted vs. asymmetrically substituted β-diketonate ligands. MCPL spectra are also reported for $EuCl_3$ dissolved in MeOH and in DMF to compare with the spectra obtained for the Eu(β-diketonate)$_3$X$_2$ complexes in these solvents.

Theory

The theory for $^7F_1 \leftarrow {}^5D_0$ MCPL in *axially* symmetric Eu(III) systems has been discussed in some detail in ref 1 and 7. The theory for $^7F_1 \leftarrow {}^5D_0$ MCPL in *nonaxially* symmetric Eu(III) systems has also been described, in a general way, in an appendix to ref 7. Anticipating the experimental results to be presented later in this paper (vide infra), we shall limit our attention here to the $^7F_1 \leftarrow {}^5D_0$ MCPL expected for systems with C_2, C_s, or C_1 symmetry. We shall not attempt to analyze the $^7F_2 \leftarrow {}^5D_0$ MCPL spectra obtained in the present study, since detailed interpretations of these spectra are somewhat more model dependent. The $^7F_{0,2} \leftarrow {}^5D_0$ transitions will only be considered with respect to the electric dipole selection rules that govern their crystal field components. It will be assumed that the intensity mechanism for the $^7F_1 \leftarrow {}^5D_0$ transition is predominantly magnetic dipole in nature.

Table I. Electric Dipole (ed) and Magnetic Dipole (md) Selection Rules for $^7F_{0,1,2} \leftarrow {}^5D_0$ Crystal Field Components in C_{4v}, C_2, and C_s Point-Group Symmetries

	crystal field components		
^7F_J	C_{4v}	C_2	C_s
$^7F_0$	$A_1 \leftarrow A_1$ (ed)	$A \leftarrow A$ (ed, md)	$A' \leftarrow A'$ (ed, md)
$^7F_1$	$A_2 \leftarrow A_1$ (md) $E \leftarrow A_1$ (ed, md)	$A \leftarrow A$ (ed, md) $2B \leftarrow A$ (ed, md)	$A' \leftarrow A'$ (ed, md) $2A'' \leftarrow A'$ (ed, md)
$^7F_2$	$A_1 \leftarrow A_1$ (ed) $B_1 \leftarrow A_1$ (f)[a] $B_2 \leftarrow A_1$ (f)[a] $E \leftarrow A_1$ (ed, md)	$3A \leftarrow A$ (ed, md) $2B \leftarrow A$ (ed, md)	$3A' \leftarrow A'$ (ed, md) $2A'' \leftarrow A'$ (ed, md)

[a] Forbidden in both electric dipole and magnetic dipole radiation.

In Table I are listed all of the crystal field components that can split out of the $^7F_{0,1,2} \leftarrow {}^5D_0$ multiplet–multiplet transitions under C_{4v}, C_2, or C_s point-group symmetry, along with designations regarding their electric and magnetic dipole allowedness. The C_{4v} selection rules are listed since it is possible (although not very probable) that the "effective" site symmetry at the Eu(III) in the systems examined here could be as high as C_{4v}. This would obtain if the bridging atoms in the chelate rings could be ignored *and* the the EuO_8 coordination cluster had a regular (undistorted) square-antiprism structure. Since the latter structure is axially symmetric, its $^7F_1 \leftarrow {}^5D_0$ MCPL could be interpreted following the arguments given in ref 1.

With reference to eq 4 of ref 1, the $H^+_{cf}(1)$ operator appropriate for either C_2 or C_s symmetry is given by

$$H^+_{cf}(1) = h^+(2,0) + h^+(2,2) \tag{1}$$

since $h^+(2,1) = 0$ in these symmetries. In this case, it is convenient to define the components of the $^7F_1$ multiplet in terms of a Cartesian basis: $|z\rangle = |{}^7F_{1,0}\rangle$, $|x\rangle = 2^{-1/2}[|{}^7F_{1,1}\rangle - |{}^7F_{1,-1}\rangle]$, and $|y\rangle = i2^{-1/2}[|{}^7F_{1,1}\rangle + |{}^7F_{1,-1}\rangle]$, where the $|{}^7F_{1,M_J}\rangle$ denote the magnetic sublevels of the $^7F_1$ multiplet. The operator $h^+(2,2)$ is diagonal in this basis with eigenvalues $E_z(2,2) = 0$ and $E_x(2,2) = -E_y(2,2) = \Delta_1(2,2)$, where $\Delta_1(2,2) = \langle x|h^+(2,2)|x\rangle$. The off-diagonal matrix elements of $h^+(2,0)$ in this basis are pure imaginary and have no influence on the $^7F_1$ energy levels. The diagonal matrix elements of $h^+(2,0)$ in this basis are given by $E_z(2,0) = \Delta_1(2,0)$ and $E_x(2,0) = E_y(2,0) = -{}^1/_2\Delta_1(2,0)$, where $\Delta_1(2,0) = \langle z|h^+(2,0)|z\rangle$. In this case, then, the $^7F_1$ multiplet is split out into three nondegenerate crystal field levels with energies

$$|z\rangle,\ E_z = E^0_1 + \Delta_1(2,0) \tag{2}$$

$$|x\rangle,\ E_x = E^0_1 - {}^1/_2\Delta_1(2,0) + \Delta_1(2,2) \tag{3}$$

$$|y\rangle,\ E_y = E^0_1 - {}^1/_2\Delta_1(2,0) - \Delta_1(2,2) \tag{4}$$

where E^0_1 denotes the energy of the unperturbed ("free-ion") multiplet level.

A nonvanishing $h^+(2,1)$ component in the crystal field will have the effect of mixing $|z\rangle$ into both $|x\rangle$ and $|y\rangle$ (and vice versa), but it will not mix $|x\rangle$ and $|y\rangle$ to first order. On the assumption that $h^+(2,1) << h^+(2,2)$, we can write (to first order in $h^+(2,1)$)

$$|z'\rangle = |z\rangle + \lambda_{zx}|x\rangle + \lambda_{zy}|y\rangle \tag{5}$$

$$|x'\rangle = |x\rangle - \lambda^*_{zx}|z\rangle \tag{6}$$

$$|y'\rangle = |y\rangle - \lambda^*_{zy}|z\rangle \tag{7}$$

(2) Kepert, D. L. *Prog. Inorg. Chem.* **1978**, *24*, 179.
(3) Sievers, R. E., Ed. "Nuclear Magnetic Resonance Shift Reagents"; Academic Press: New York, 1973.
(4) Horrocks, W. D., Jr.; Sipe, J. P. *Science (Washington, D.C.)* **1972**, *177*, 994.
(5) Horrocks, W. D., Jr. *J. Am. Chem. Soc.* **1974**, *96*, 3022.
(6) Horrocks, W. D., Jr.; Sipe, J. P.; Sudnick, D. In "Nuclear Magnetic Resonance Shift Reagents"; Sievers, R. E., Ed.; Academic Press: New York, 1973; pp 53–86.
(7) Richardson, F. S.; Brittain, H. G. *J. Am. Chem. Soc.* **1981**, *103*, 18.

where λ_{zx} and λ_{zy} are first-order perturbation coefficients. The energies of these perturbed levels are given by

$$E_{z'} = E_1^0 + \Delta_1(2,0) - E_x'' - E_y'' \quad (8)$$

$$E_{x'} = E_1^0 - \tfrac{1}{2}\Delta_1(2,0) + \Delta_1(2,2) + E_x'' \quad (9)$$

$$E_{y'} = E_1^0 - \tfrac{1}{2}\Delta_1(2,0) - \Delta_1(2,2) + E_y'' \quad (10)$$

where

$$E_x'' = \frac{|\langle x|h^+(2,1)|z\rangle|^2}{\Delta_1(2,2) - \tfrac{3}{2}\Delta_1(2,0)} \quad (11)$$

$$E_y'' = \frac{|\langle y|h^+(2,1)|z\rangle|^2}{-\Delta_1(2,2) - \tfrac{3}{2}\Delta_1(2,0)} \quad (12)$$

The total (unpolarized) emission associated with each of the $^7F_{1,i} \leftarrow {}^5D_0$ transitions (where $i = x$, y, and z *or* x', y', and z') can be described by

$$I/E = K\nu_{i0}^3\, \bar{D}_0(i\leftarrow 0)\, f_{i0}(E) \quad (13)$$

where E denotes photon energy, ν_{i0} is the $i \leftarrow 0$ transition frequency, $f_{i0}(E)$ is a normalized line-shape function centered at ν_{i0}, $K = 8\pi^3 N_e/c^3$ (where N_e denotes the steady-state population of the $^5D_0$ emitting level) and $\bar{D}_0$ $(i\leftarrow 0)$ is a magnetic dipole strength defined by

$$\bar{D}_0(i\leftarrow 0) = \tfrac{1}{3}|\langle {}^7F_{1,i}|\mathbf{m}|{}^5D_0\rangle|^2 \quad (14)$$

Since, in the absence of significant J–J' mixing, $\bar{D}_0(i\leftarrow 0)$ will have the same values for $i = x$, y, and z (*or* x', y', and z'), one may expect to observe three emission lines of approximately equal intensity in the $^7F_1 \leftarrow {}^5D_0$ transition region. The energies of these lines are given by

$$h\nu_{z'0} = \Delta E_{10}^0 - \Delta_1(2,0) + E_x'' + E_y'' \quad (15)$$

$$h\nu_{x'0} = \Delta E_{10}^0 + \tfrac{1}{2}\Delta_1(2,0) - \Delta_1(2,2) - E_x'' \quad (16)$$

$$h\nu_{y'0} = \Delta E_{10}^0 + \tfrac{1}{2}\Delta_1(2,0) + \Delta_1(2,2) - E_y'' \quad (17)$$

where ΔE_{10}^0 is the difference in baricenter energies for the $^7F_1$ and $^5D_0$ multiplets.

With the assumption of linearity in the relationship between ΔI and magnetic field strength $|\mathbf{B}|$, the MCPL (ΔI vs. E) associated with each of the $^7F_{1,i} \leftarrow {}^5D_0$ transitions can be described by

$$\Delta I/E = -K\nu_{i0}^3\mu_B|\mathbf{B}|\bar{B}_0(i\leftarrow 0)\, f_{i0}(E) \quad (18)$$

where μ_B is the Bohr magneton and $\bar{B}_0$ is an orientationally averaged Faraday B parameter.[1] On the assumption that the Zeeman operator associated with the externally applied magnetic field operates only *within* the $^7F_1$ multiplet, the $\bar{B}_0(i\leftarrow 0)$ parameter can be expressed as

$$\bar{B}_0(i\leftarrow 0) = -(2/3\mu_B)\ \mathrm{Im} \sum_{j\neq i} [\langle {}^7F_{1,i}|\mathbf{m}|{}^7F_{1,j}\rangle \cdot \langle {}^5D_0|\mathbf{m}|{}^7F_{1,i}\rangle \times \langle {}^7F_{1,j}|\mathbf{m}|{}^5D_0\rangle](E_j - E_i)^{-1} \quad (19)$$

where $j = x$, y, and z (*or* z', y', and z'). The $\Delta I/I$ ratios predicted for the $^7F_{1,i} \leftarrow {}^5D_0$ component transitions are given by

$$\Delta I/I = -\mu_B|\mathbf{B}|\bar{B}_0(i\leftarrow 0)/\bar{D}_0(i\leftarrow 0) \quad (20)$$

In the special case where $h^+(2,0) = h^+(2,1) = 0$ and $|\Delta_1(2,2)| >> |g\mu_B\mathbf{B}|$, we obtain the results $\bar{B}_0(z\leftarrow 0) = 0$ and $\bar{B}_0(x\leftarrow 0) = -\bar{B}_0(y\leftarrow 0)$. In this case, we expect to observe just *two* circularly polarized emission lines (with oppositely signed ΔI values), one at $h\nu_{x0} \cong \Delta E_{10}^0 - \Delta_1(2,2)$ and one at $h\nu_{y0} \cong \Delta E_{10}^0 + \Delta_1(2,2)$. The $z \leftarrow 0$ line at $h\nu_{z0} = E_{10}^0$ will be unpolarized. The total (unpolarized) emission spectrum will show three equally spaced lines with nearly identical intensities, while the MCPL spectrum will exhibit two lines with ΔI values that are equal in magnitude but opposite in sign. That is

$$I/E = K\bar{D}_0(z\leftarrow 0)[\nu_{x0}^3 f_{x0}(E) + \nu_{y0}^3 f_{y0}(E) + \nu_{z0}^3 f_{z0}(E)] \quad (21)$$

$$\Delta I/E = K\mu_B|\mathbf{B}|\bar{B}_0(x\leftarrow 0)[\nu_{y0}^3 f_{y0}(E) - \nu_{x0}^3 f_{x0}(E)] \quad (22)$$

Relaxation of the $h^+(2,0) = h^+(2,1) = 0$ condition, so that either or both of the $h^+(2,0)$ and $h^+(2,1)$ crystal field components are nonzero, has the effect of making the $z \leftarrow 0$ transition partially (circularly) polarized. That is, $\bar{B}_0(z\leftarrow 0)$ becomes nonvanishing. Furthermore, since the sum rule, $\sum_i \bar{B}_0(i\leftarrow 0) = 0$, must be satisfied (in the absence of J–J' mixings), we also have $\bar{B}_0(x\leftarrow 0) + \bar{B}_0(y\leftarrow 0) = -\bar{B}_0(z\leftarrow 0)$. In this case, we may expect to observe three MCPL lines in the $^7F_1 \leftarrow {}^5D_0$ transition region.

In addition to the crucial role played by the $h^+(2,q)$ operators in determining the detailed emission properties of the $^7F_1 \leftarrow {}^5D_0$ transition, these operators are also largely responsible for any electric dipole intensity observed in the $^7F_0 \leftarrow {}^5D_0$ transition. According to the Judd–Ofelt[8,9] intensity theory for 4f $\leftrightarrow$ 4f transitions, $^7F_0 \leftarrow {}^5D_0$ is strictly electric dipole forbidden in the absence of J–J' mixing. More particularly, to exhibit electric dipole intensity, this transition must acquire some $|\Delta J| = 2$, 4, or 6 character via $(J = 0)$–$(J' = 2, 4,$ or 6) multiplet–multiplet mixing. Most effective in this regard are $^7F_0$–$^7F_2$ and $^5D_0$–$^5D_2$ mixings promoted by the $h^+(2,q)$ components of the crystal field potential. As will be seen later (vide infra), several of the systems examined in this study exhibit remarkably intense $^7F_0 \leftarrow {}^5D_0$ emissions, indicative of strong $h^+(2,q)$ crystal field components.

One final point of theory concerns the magnetic dipole allowedness of the $^7F_0 \leftarrow {}^5D_0$ transition. This transition can acquire magnetic dipole intensity only to *at least* second order in the H_{cf}^+ crystal field Hamiltonian in the absence of an applied magnetic field. However, in the presence of an applied field, the Zeeman operator H_{ze} can mix $^7F_0$ with $^7F_1$ $(M_J = 0)$ and $^5D_0$ with $^5D_1$ $(M_J = 0)$, thereby giving some $\Delta J = \pm 1$ $(\Delta M_J = 0)$ character to the perturbed $^7F_0 \leftarrow {}^5D_0$ transition. This satisfies the intermediate-coupling selection rules for magnetic dipole allowedness, and therefore, one may predict a field-dependent $^7F_0 \leftarrow {}^5D_0$ magnetic dipole intensity. In a perturbation theory context, the $^7F_0 \leftarrow {}^5D_0$ transition can "steal" magnetic dipole intensity from the $^7F_1(M_J = 0) \leftarrow {}^5D_0$ transition under the influence of the applied magnetic field.

Experimental Section

Spectroscopic Measurements. The magnetic circularly polarized luminescence (MCPL) experiments were carried out with the samples contained in an insulated cell placed in the bore of a superconducting magnet (Oxford Instruments). Sample temperature was maintained at ~296 K in all experiments. Sample luminescence was excited with the 466-nm line of a CW argon ion laser, and the MCPL and total luminescence spectra were recorded simultaneously on an emission spectrophotometer constructed in this laboratory. Magnetic field strengths were varied between 0 and 4.2 T. All MCPL spectra are displayed as ΔI vs. $\bar{\nu}$ (cm^{-1}) plots, where $\Delta I = I_L - I_R$, and all total luminescence spectra are displayed as $I/2$ vs. $\bar{\nu}$ (cm^{-1}) plots, where $I = I_L + I_R$. Both ΔI and I are scaled in arbitrary units.

(8) Judd, B. R.. *Phys. Rev.* **1962**, *127*, 750.
(9) Ofelt, G. S. *J. Chem. Phys.* **1962**, *37*, 511.
(10) Kirby, A. F.; Foster, D. R.; Richardson, F. S. *Chem. Phys. Lett.* **1983**, *95*, 507.
(11) Kirby, A. F.; Richardson, F. S. *J. Phys. Chem.* **1983**, *87*, 2544, 2557.
(12) Mason, S. F.; Peacock, R. D.; Stewart, B. *Mol. Phys.* **1975**, *30*, 1829.
(13) Mason, S. F. *Struct. Bonding (Berlin)* **1980**, *39*, 43.
(14) Peacock, R. D. *Struct. Bonding (Berlin)* **1975**, *22*, 83.
(15) Brittain, H. G.; Richardson, F. S. *J. Am. Chem. Soc.* **1976**, *98*, 5858.

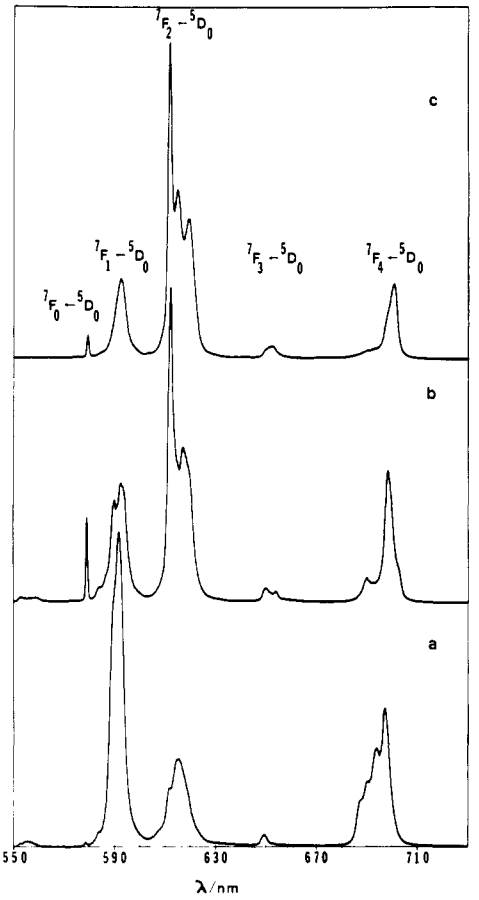

Figure 1. Unpolarized emission spectra for 0.10 M solutions of $EuCl_3$ in D_2O (a), MeOH (b), and DMF (c) (λ_{ex} = 395 nm, $\Delta\lambda_{em}$ = 0.5 nm; no magnetic field). The intensity scales are in arbitrary units.

All MCPL measurements reported here were carried out on solution samples in which the solvent was either anhydrous methanol (MeOH) or anhydrous *N*,*N*-dimethylformamide (DMF). The $EuCl_3$/MeOH and $EuCl_3$/DMF samples were each 0.10 M in the anhydrous $EuCl_3$ salt. All other samples were 0.03 M in the europium(III) chelate. The five chelate systems (designated as compounds **1**–**5**) examined in this study are depicted in Chart I.

Preparation of Complexes. The reagents $EuCl_3 \cdot nH_2O$ (Apache Chemicals), 1,10-phenanthroline (G. F. Smith), and triethanolamine (Baker Analyzed reagent) were purchased and used without further purification. The reagents 1,1,1,5,5,5-hexafluoro-2,4-pentanedione, 1,1,1-trifluoro-2,4-pentanedione, and 4,4,4-trifluoro-1-(2-furyl)-1,3-butanedione (Eastman-Kodak) were distilled before use. The reagent 1,3-bis(3-pyridyl)-1,3-propanedione (cream-colored needles, mp 198 °C) was prepared by an adaptation of the method of Kuick and Adkins.[16]

Compound **1**, tris[1,1,1,5,5,5-hexafluoro-2,4-pentanedionato]europium(III), compound **2**, tris[1,1,1-trifluoro-2,4-pentanedionato]europium(III), compound **3**, tris[1,3-bis(3-pyridyl)-1,3-propanedionato]europium(III), and compound **4**, tris[4,4,4-trifluoro-1-(2-furyl)-1,3-butanedionato]europium(III), were each prepared by the general method of Charles and Riedel,[17] with triethanolamine instead of piperidine as the base. From the original aqueous ethanol reaction mixture, compounds **3** and **4** were obtained in crystalline form as the dihydrates, whereas compounds **1** and **2** separated as monohydrates. The anhydrous forms of compounds **1**–**4** could be obtained by drying under vacuum over KOH or by recrystallizing from a nonaqueous solvent.

Compound **5**, tris[4,4,4-trifluoro-1-(2-furyl)-1,3-butanedionato](1,10-phenanthroline)europium(III), was prepared by the method of Melby et al.[18]

(16) Kuick, L. F.; Adkins, H. *J. Am. Chem. Soc.* **1935**, *57*, 143.
(17) Charles, R. G.; Riedel, E. P. *J. Inorg. Nucl. Chem.* **1967**, *29*, 715.
(18) Melby, L. R.; Rose, N. J.; Abramson, E.; Caris, J. C. *J. Am. Chem. Soc.* **1964**, *86*, 5117.

Chart I

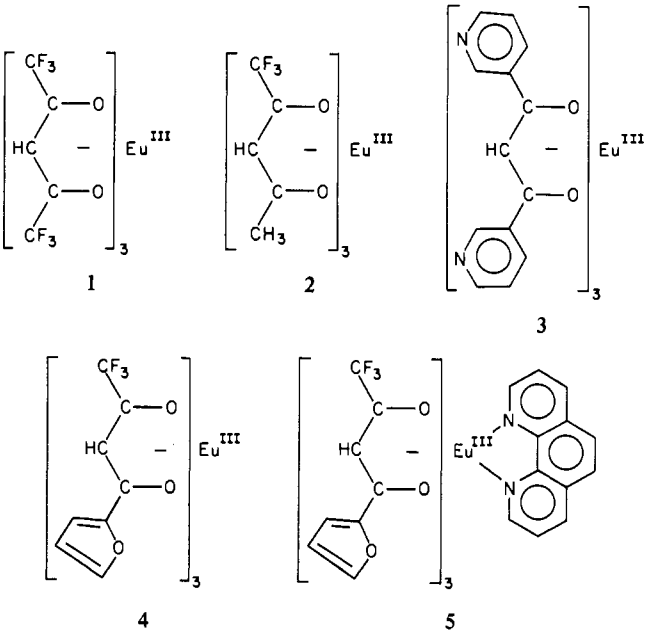

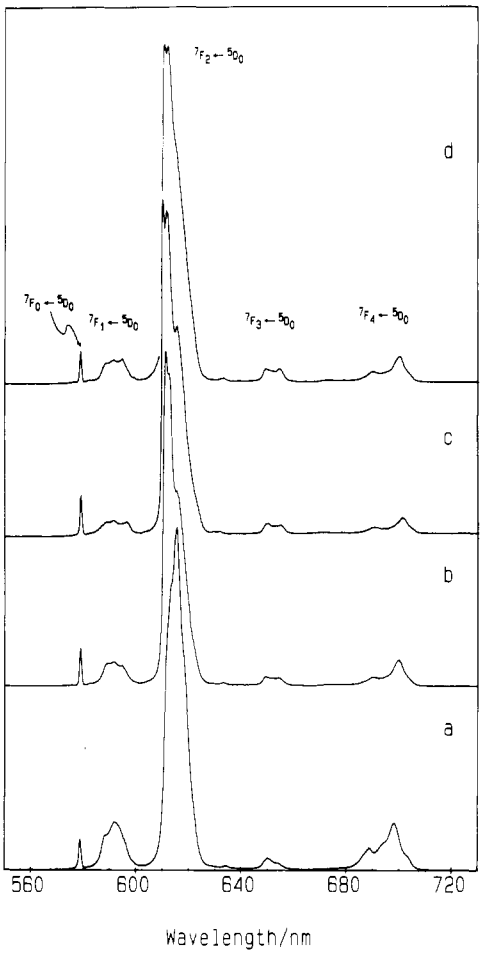

Figure 2. Unpolarized emission spectra for 0.03 M solutions of compounds **1** (a), **2** (b), **3** (c), and **4** (d) in DMF (λ_{ex} = 395 nm, $\Delta\lambda_{em}$ = 0.5 nm; no magnetic field). The intensity scales are in arbitrary units.

Results

Unpolarized emission spectra obtained in the absence of an applied magnetic field are shown in Figure 1 for $EuCl_3$ dissolved in D_2O, MeOH, and DMF, with $[Eu^{3+}]$ = 0.10 M.

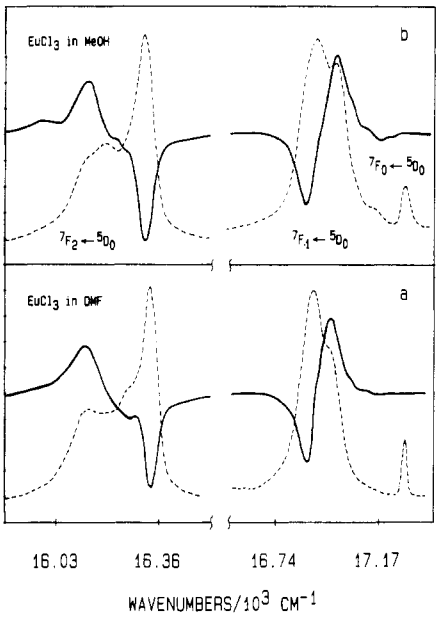

Figure 3. MCPL (ΔI, solid-line spectra) and total luminescence (I, dashed-line spectra) in the $^7F_{0,1} \leftarrow {}^5D_0$ and $^7F_2 \leftarrow {}^5D_0$ transition regions for $EuCl_3$ in DMF (a) and in MeOH (b) with [$EuCl_3$] = 0.10 M (B = 4.2 T, λ_{ex} = 466 nm, $\Delta\lambda_{em}$ = 2 nm). The intensity scales are in arbitrary units.

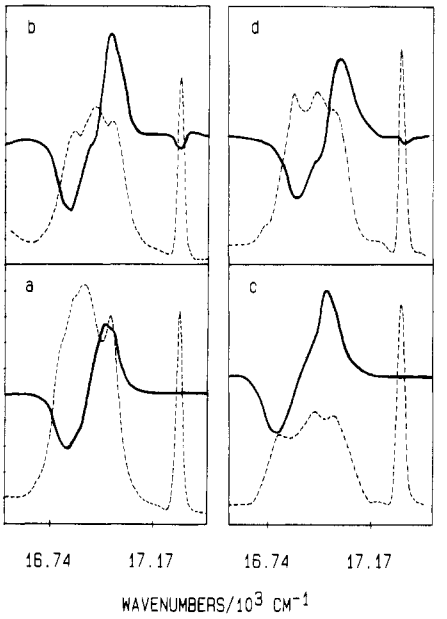

Figure 4. MCPL (ΔI, solid-line spectra) and total luminescence (I, dashed-line spectra) in the $^7F_{0,1} \leftarrow {}^5D_0$ transition regions for compounds **1** (a), **2** (b), **3** (c), and **4** (d) in DMF with [chelate] = 0.03 M (B = 4.2 T, λ_{ex} = 466 nm, $\Delta\lambda_{em}$ = 2 nm). The intensity scales are in arbitrary units.

These are *corrected* emission spectra obtained with a spectral resolution of ~0.5 nm at 600 nm. Of special note in these spectra are the *relative* intensities of the $^7F_{0,1,2,3,4} \leftarrow {}^5D_0$ emissions as a function of solvent. All of these spectra were obtained on an SLM photon-counting emission spectrophotometer with excitation centered at 395 nm ($^7F_0 \rightarrow {}^5D_3$ Eu^{3+} absorption).

Unpolarized emission spectra obtained in the absence of an applied magnetic field are shown in Figure 2 for compounds **1**–**4** dissolved in DMF, with [chelate] = 0.03 M. These spectra were obtained under the same spectral conditions noted above for the $EuCl_3$ salt dissolved in various solvents.

MCPL (ΔI) and total luminescence (I) spectra obtained in the presence of an applied magnetic field (B = 4.2 T) are shown in Figure 3 for $EuCl_3$ in MeOH and in DMF. These spectra were obtained with a spectral resolution of ~2 nm (at 600 nm) and 466-nm laser excitation (corresponding to $^7F_0 \rightarrow {}^5D_2$ Eu^{3+} absorption). The lower resolution achieved for these spectra, vs. that achieved for the spectra shown in Figure 1, is due to the difficulties attendant with collecting sample emission when the sample is located in the magnet system. The consequent lower emission intensities achievable in the MCPL experiments required the use of wider slit widths in the emission monochromator. With the exception of some very slight band narrowing, the zero-field (B = 0) total luminescence (I) spectra obtained for $EuCl_3$ in MeOH and in DMF are identical with the B = 4.2 T total luminescence spectra shown in Figure 3. This indicates that the nonspherical components of the crystal field potential exert a stronger influence on the 4f-electron states than does the applied magnetic field (i.e., $H_{cf}^{+} >> H_{ze}$).

MCPL (ΔI) and total luminescence (I) spectra obtained at B = 4.2 T are shown in Figures 4 and 5 for compounds **1**–**4** in DMF and in Figure 6 for compounds **1** and **2** in MeOH. The MCPL and total luminescence spectra obtained for compound **5** in DMF are shown in Figure 7.

The ΔI and I intensity scales in Figures 3–7 are in arbitrary units, and these spectra are *uncorrected* with respect to the wavelength-dependent sensitivity of the emission detection system of our spectrophotometer. In making comparisons between the *relative* emission intensities of the $^7F_J \leftarrow {}^5D_0$ transitions, one needs to refer to the *corrected* emission spectra shown in Figures 1 and 2.

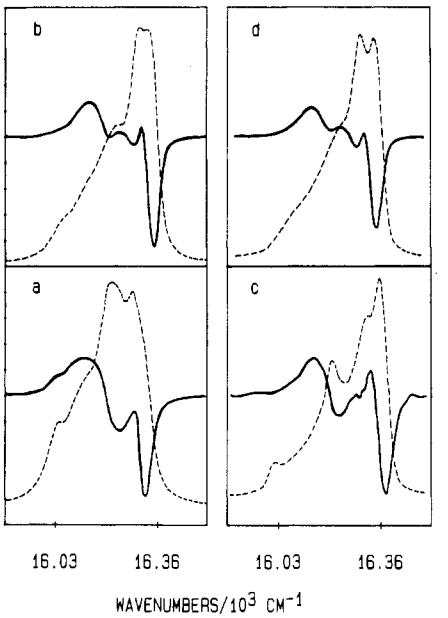

Figure 5. MCPL (ΔI, solid-line spectra) and total luminescence (I, dashed-line spectra) in the $^7F_2 \leftarrow {}^5D_0$ transition region for compounds **1** (a), **2** (b), **3** (c), and **4** (d) in DMF with [chelate] = 0.03 M (B = 4.2 T, λ_{ex} = 466 nm, $\Delta\lambda_{em}$ = 2 nm). The intensity scales are in arbitrary units.

Discussion

$EuCl_3$. On the assumption that the oscillator strength of the $^7F_1 \leftarrow {}^5D_0$ transition remains relatively constant (independent of the structural details of the ligand environment),[1,10,11] the spectra of Figure 1 demonstrate the strong sensitivity of the $^7F_{0,2,4} \leftarrow {}^5D_0$ emission intensities to the ligand field about the Eu^{3+} ion. The ratio of $^7F_2 \leftarrow {}^5D_0$ vs. $^7F_1 \leftarrow {}^5D_0$ intensities is seen to increase dramatically on going from D_2O to DMF, with the result for MeOH falling between (but

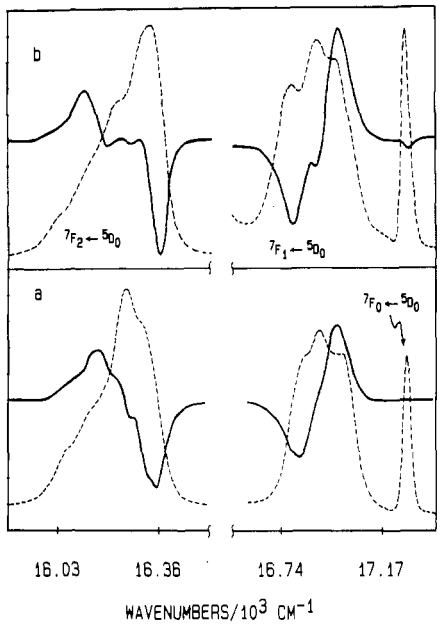

Figure 6. MCPL (ΔI, solid-line spectra) and total luminescence (I, dashed-line spectra) in the $^7F_{0,1} \leftarrow {}^5D_0$ and $^7F_2 \leftarrow {}^5D_0$ transition regions for compounds **1** (a) and **2** (b) in MeOH with [chelate] = 0.03 M (B = 4.2 T, λ_{ex} = 466 nm, $\Delta\lambda_{em}$ = 2 nm). The intensity scales are in arbitrary units.

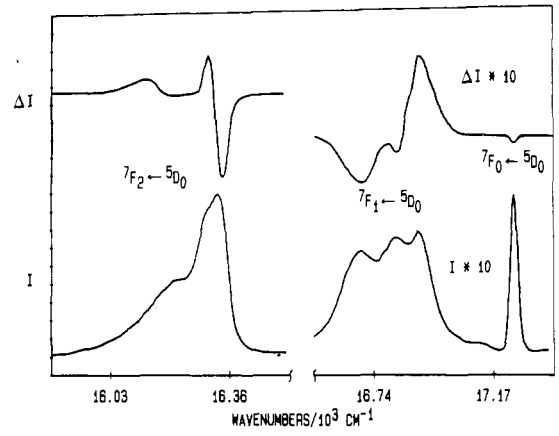

Figure 7. MCPL (ΔI) and total luminescence (I) spectra for compound **5** in DMF with [chelate] = 0.03 M (B = 4.2 T, λ_{ex} = 466 nm, $\Delta\lambda_{em}$ = 2 nm).

closer to that for DMF). This follows what is expected from the ligand dipolar polarization model for $^7F_2 \leftarrow {}^5D_0$ "hypersensitivity". According to this model, the oscillator strength of the $^7F_2 \leftarrow {}^5D_0$ transition should be proportional to the square of the ligand dipolar polarizability.[12,13] With respect to the latter property, we have the following order for the solvent molecules (ligands) represented in the spectra of Figure 1: $\bar{\alpha}$(DMF) > $\bar{\alpha}$(MeOH) > $\bar{\alpha}$(D_2O).

The $^7F_1 \leftarrow {}^5D_0$ MCPL spectra shown in Figure 3 suggest that the major structural species present in both MeOH and DMF solutions of $EuCl_3$ are axially symmetric. In both cases, the lower frequency component of the $^7F_1 \leftarrow {}^5D_0$ total luminescence spectrum can be assigned to $\Delta M_J = \pm 1$ transitions, while the higher frequency component can be assigned to the $\Delta M_J = 0$ transition. The latter appears only as a shoulder in the spectrum for $EuCl_3$ in DMF (see Figure 3). The appearance of substantial $^7F_2 \leftarrow {}^5D_0$ intensity in the spectra for $EuCl_3$ in MeOH and in DMF rules out the predominance of centrosymmetric coordination species, and the appearance of substantial $^7F_0 \leftarrow {}^5D_0$ intensity also rules out coordination species of either D_{4d} or D_{3h} symmetry. The latter two symmetry types would apply respectively to 8-coordinate regular square-antiprism structures (D_{4d}) and to 9-coordinate regular tricapped-trigonal-prism structures (D_{3h}). The $EuCl_3$(aquo) spectrum is entirely compatible with the dominance of 9-coordinate D_{3h} structures. Considering all three $^7F_{2,1,0} \leftarrow {}^5D_0$ emission regions for $EuCl_3$ in MeOH and in DMF, the spectra suggest the dominance of C_{3v} structural types. This would be compatible with 7-coordinate complexes having monocapped-distorted-octahedral structures. In C_{3v} symmetry, the $^7F_0 \leftarrow {}^5D_0$ transition is electric dipole allowed and the $^7F_2 \leftarrow {}^5D_0$ transition can split into three electric dipole allowed components, two of which are doubly degenerate and also magnetic dipole allowed. The $^7F_1 \leftarrow {}^5D_0$ transition would split into two magnetic dipole allowed components, one of which is double degenerate and also electric dipole allowed. These C_{3v} selection rules are compatible with the total luminescence spectra observed for $EuCl_3$ in MeOH and in DMF (see Figures 1 and 3).

Eu(β-diketonate)$_3$X$_2$ Complexes. Compounds **1–4** differ (chemically) *only* with respect to the substituents on the β-diketonate ligands (see Chart I). It is clear from the emission spectra shown in Figure 2, however, that the nature and number of ligand substituents can influence both the relative intensities and the splitting patterns (or band shapes) observed in the $^7F_J \leftarrow {}^5D_0$ emission regions. Each of these compounds in both MeOH and DMF exhibit substantial $^7F_0 \leftarrow {}^5D_0$ emission intensity (see Figures 2, 4, 6, and 7), and for **3** the total (integrated) intensity of this transition is observed to be comparable to that of the $^7F_1 \leftarrow {}^5D_0$ transition. This suggests substantial $^7F_0$–$^7F_2$ (and, possibly, $^5D_0$–$^5D_2$) multiplet–multiplet mixings due to strong $h^+(2,q)$ crystal field components. Such multiplet–multiplet mixings can enhance the electric dipole intensity of the $^7F_0 \leftarrow {}^5D_0$ transition via the $|\Delta J| = 2$ electric dipole selection rule.[14] Further evidence that the $h^+(2,q)$ components of the crystal field are quite strong is the observation that the total luminescence spectra in the $^7F_1 \leftarrow {}^5D_0$ transition region are essentially independent of magnetic field strength from B = 0 to B = 4.2 T. That is, the energies of the $^7F_1$ crystal field levels (as determined by $h^+(2,q)$) are not much affected by H_{ze}.

The $I(^7F_0 \leftarrow {}^5D_0)$:$I(^7F_1 \leftarrow {}^5D_0)$ and $I(^7F_2 \leftarrow {}^5D_0)$:$I(^7F_1 \leftarrow {}^5D_0)$ intensity ratios exhibit similar variations among compounds **1–4** (in both MeOH and DMF). They follow the order **3** > **4** > **2** > **1**. On the assumption that the $^7F_1 \leftarrow {}^5D_0$ oscillator strength will be essentially the same for each of these compounds, variations in the $I(^7F_{0,2} \leftarrow {}^5D_0)$:$I(^7F_1 \leftarrow {}^5D_0)$ ratios can be interpreted in terms of ligand-dependent $^7F_2 \leftarrow {}^5D_0$ electric dipole oscilltor strengths. Among the ligand substituents found in compounds **1–4**, the pyridyl substituents in **3** and the furyl substituent in **4** are the most polarizable and, according to the ligand dipolar polarization model,[11-14,19,20] should induce more electric dipole intensity in the $^7F_2 \leftarrow {}^5D_0$ transition than the less polarizable CF_3 and CH_3 substituents found in compounds **1** and **2**. This would account for the larger $I(^7F_{0,2} \leftarrow {}^5D_0)$:$I(^7F_1 \leftarrow {}^5D_0)$ ratios observed for **3** and **4** vs. those observed for **1** and **2**. The significant differences observed between the spectra of **1** and **2** (in intensity ratios *and* band splitting patterns) may reflect the differences in the substitutional symmetry for the respective ligands. In **1**, the ligands are symmetrically substituted whereas, in **2**, the ligands are asymmetrically substituted (see Chart I). The latter compound exhibits the greater $I(^7F_{0,2} \leftarrow {}^5D_0)$:$I(^7F_1 \leftarrow {}^5D_0)$ intensity ratios and the larger splitting within the $^7F_1 \leftarrow {}^5D_0$ emission band.

The total (unpolarized) emission spectra obtained in the $^7F_{0,1} \leftarrow {}^5D_0$ transition regions for compounds **1–4** exhibit no magnetic field dependence from B = 0 to B = 4.2 T. The

(19) Richardson, F. S. *Chem. Phys. Lett.* **1982**, *86*, 47.
(20) Reid, M. F.; Richardson, F. S. *Chem. Phys. Lett.* **1983**, *95*, 501.

number and locations of lines, as well as the *relative* line intensities, are independent of field strength. In both MeOH and DMF, a single sharp line is observed for the $^7F_0 \leftarrow {}^5D_0$ transition (at ~17 274 cm^{-1}), and in each case the $^7F_1 \leftarrow {}^5D_0$ emission can be resolved into three lines of approximately equal intensity. The spacings between the three $^7F_1 \leftarrow {}^5D_0$ component lines vary from compound to compound, and they also show a weak solvent dependence. The appearance of three lines in the *zero-field* $^7F_1 \leftarrow {}^5D_0$ emission spectra, and of just a single line in the $^7F_0 \leftarrow {}^5D_0$ emission region, provides evidence for a homogeneous sample of nonaxially symmetric structures. That is, it suggests that only one type of structural species is present in solution and that this species is nonaxially symmetric.

The $^7F_1 \leftarrow {}^5D_0$ MCPL spectra displayed in Figures 4 and 6 show that both the high-energy and low-energy components of this transition are strongly circularly polarized (large values of $|\Delta I/I|$), while the middle component is only weakly circularly polarized (small value for $|\Delta I/I|$). This means that the high-energy and low-energy components have predominantly $\Delta M_J = \pm 1$ character, whereas the middle component has predominantly $\Delta M_J = 0$ character. From our discussion in the Theory section, we see that this is precisely what would be expected for the case where $h^+(2,2)$ is the dominant term in the $H_{cf}^+(1)$ crystal field Hamiltonian (see eq 4 of Ref 1). The high-energy and low-energy components can be assigned, therefore, as field-induced mixtures of the $^7F_{1x'} \leftarrow {}^5D_0$ and $^7F_{1y'} \leftarrow {}^5D_0$ transitions, and the middle component can be assigned to the $^7F_{1z'} \leftarrow {}^5D_0$ transition. If we set $h^+(2,0) = h^+(2,1) = 0$, and assume that $H_{cf}^+ >> H_{ze}$ within the $^7F_1$ multiplet, then from eq 15–17 the transition energies of the three components are predicted to be $\Delta E_{10}^0 \pm \Delta_1(2,2)$ and ΔE_{10}^0. In this case, the $^7F_1 \leftarrow {}^5D_0$ MCPL spectrum would be described by eq 22, and one would observe just two bands, opposite in sign and equal in intensity, located at $\Delta E_{10}^0 \pm \Delta_1(2,2)$. Although this comes close to matching the observed MCPL spectra, it does *not* account for the very weak ΔI signals observed in the middle component of the $^7F_1 \leftarrow {}^5D_0$ transition.

Now let us assume $h^+(2,2) > h^+(2,0) \neq 0$, $h^+(2,1) = 0$, and $H_{cf}^+(1) >> H_{ze}$. In this case, the transition energies of the three $^7F_1 \leftarrow {}^5D_0$ components are predicted to be $\Delta E_{10}^0 + {}^1/_2\Delta_1(2,0) \pm \Delta_1(2,2)$ and $\Delta E_{10}^0 - \Delta_1(2,0)$. The high- and low-energy components are displaced from the middle component by ${}^3/_2\Delta_1(2,0) \pm \Delta_1(2,2)$ and from each other by $2\Delta_1(2,2)$. Furthermore, the middle component ($^7F_{1z} \leftarrow {}^5D_0$) can become partially circularly polarized, exhibiting an MCPL (ΔI) signal whose sign will depend upon the signs of the $\Delta_1(2,0)$ and $\Delta_1(2,2)$ energy parameters. So long as $h^+(2,2) > h^+(2,0)$, the $^7F_{1x} \leftarrow {}^5D_0$ and $^7F_{1y} \leftarrow {}^5D_0$ components will exhibit relatively large $\Delta I/I$ values (of opposite signs), while the $|\Delta I/I|$ associated with the $^7F_{1z} \leftarrow {}^5D_0$ component will be small. All of the $^7F_1 \leftarrow {}^5D_0$ MCPL spectra shown in Figures 4 and 6 for compounds **1–4** appear to fit this case where $h^+(2,2) > h^+(2,0) \neq 0$ and $h^+(2,1)$ is assumed to be negligibly small. With the assumption of this model, the following relationships can be used to deduce the absolute magnitude of the second-order orthorhombic crystal field coefficient, $B_2^{(2)}$:

$$|h\nu_{x0} - h\nu_{y0}| = 2|\Delta_1(2,2)| = (4/5)^{1/2}|B_2^{(2)}(^7F_1||U^{(2)}||^7F_1)| \quad (23)$$

where $B_2^{(2)}$ has been defined in the unit-tensor normalization scheme[21] and $(^7F_1||U^{(2)}||^7F_1)$ is the reduced matrix element of the $U^{(2)}$ operator within the $^7F_1$ multiplet. When $^7F_1$ is taken to be a pure Russell–Saunders state, the reduced matrix element in eq 23 is readily evaluated to yield a value of $(9/56)^{1/2}$. It follows that

$$|B_2^{(2)}| = (70/9)^{1/2}|h\nu_{x0} - h\nu_{y0}| \quad (24)$$

Empirically determined values for $|B_2^{(2)}|$ are listed in Table II.

Table II. Empirically Determined Values for $|B_2^{(2)}|$[a]

compd	solvent	$\lvert B_2^{(2)}\rvert$, cm^{-1}	compd	solvent	$\lvert B_2^{(2)}\rvert$, cm^{-1}
1	DMF	516	4	DMF	499
	MeOH	480		MeOH	516
2	DMF	466	5	DMF	601
	MeOH	514		MeOH	600
3	DMF	632			
	MeOH	513			

[a] Determined from eq 24 by using the data presented in Figures 4, 6, and 7.

An analysis of the $^7F_2 \leftarrow {}^5D_0$ MCPL spectra would require the simultaneous consideration of all $h^+(2,q)$ *and* $h^+(4,q)$ components of the crystal field. This is beyond the scope of the present study.

Eu(β-diketonate)$_3$(*o*-phen). This complex (**5**) is unique among the systems examined in this study since it can accomodate solvent molecules in its inner coordination sphere *only* by becoming at least 9-coordinate. In fact, no solvent dependence was observed in the spectra obtained for this system, and its total luminescence spectra were observed to be *field independent*. The relatively large $I(^7F_0 \leftarrow {}^5D_0):I(^7F_1 \leftarrow {}^5D_0)$ and $I(^7F_2 \leftarrow {}^5D_0):I(^7F_1 \leftarrow {}^5D_0)$ intensity ratios observed in the spectra of this system reflect the presence of several highly polarizable ligand moieties, as predicted by the ligand dipolar polarization intensity model.[11-14]

The $^7F_1 \leftarrow {}^5D_0$ MCPL spectrum of **5** in DMF (see Figure 7) matches almost exactly that predicted for a system in which $h^+(2,2) >> h^+(2,0)$ and in which $h^+(2,1)$ is negligibly small. Assigning the weak center band in the MCPL spectrum to the $\Delta M_J = 0$ component of the $^7F_1 \leftarrow {}^5D_0$ transition and the two sidebands to the predominantly $\Delta M_J = \pm 1$ components, we estimate the magnitude of $\Delta_1(2,2)$ to be ~108 cm^{-1}.

Conclusions

The total luminescence (I) and MCPL (ΔI) spectra for $EuCl_3$ in both MeOH and DMF indicate axially symmetric coordination species, with the details of these spectra suggesting that these species have C_{3v} point-group symmetry. The spectra obtained for the five Eu(β-diketonate)$_3$ complexes (compounds **1–5**) in both MeOH and DMF show that these complexes (or the corresponding chelate–solvent adduct species) each exists as a predominantly nonaxially symmetric structure in which $h^+(2,2) > h^+(2,0)$.

Small solvent effects (DMF vs. MeOH) were observed in the spectra of each of the tris chelate systems (**1–4**). These effects appeared in the *relative* $^7F_{0,1,2} \leftarrow {}^5D_0$ emission intensities and in the splitting patterns (and energies) observed within the $^7F_1 \leftarrow {}^5D_0$ and $^7F_2 \leftarrow {}^5D_0$ transition regions. On the other hand, no solvent effects were observed in the spectra obtained on the 8-coordinate Eu(β-diketonate)$_3$(*o*-phen) system (**5**).

The *relative* intensities of the $^7F_2 \leftarrow {}^5D_0$ and $^7F_1 \leftarrow {}^5D_0$ emissions were observed to be very sensitive to the structural details and chemical nature of the ligand environment, with large $I(^7F_2 \leftarrow {}^5D_0):I(^7F_1 \leftarrow {}^5D_0)$ ratios correlating closely with the presence of highly polarizable ligands or ligand substituents. The latter observation lends support to the ligand dipolar polarization model for 4f → 4f intensities, insofar as this model predicts that the electric dipole intensity of the $^7F_2 \leftarrow {}^5D_0$ Eu^{3+} transition should be especially sensitive to ligand polarizability. The $I(^7F_0 \leftarrow {}^5D_0):I(^7F_1 \leftarrow {}^5D_0)$ intensity ratios were also found

(21) Wybourne, B. G. "Spectroscopic Properties of Rare Earths"; Wiley-Interscience: New York, 1965.

to correlate closely with ligand polarizability, as well as with the apparent magnitudes of the $h^+(2,q)$ crystal field components. This can be interpreted as due to intensity "borrowing" by the $^7F_0 \leftarrow {}^5D_0$ transition from the $^7F_2 \leftarrow {}^5D_0$ transition via crystal field induced mixings between the $^7F_0$ and $^7F_2$ (and $^5D_0$ and $^5D_2$) multiplet states. To first order, such mixings would arise from the $h^+(2,q)$ components of the crystal field potential.

Acknowledgment. This work was supported by grants from the National Science Foundation (NSF Grant CHE80-04209 to F.S.R.) and the National Institutes of Health (Grant R01-CA-30148 to L.M.V.).

Registry No. **1**, 14592-81-5; **2**, 14526-21-7; **3**, 87616-08-8; **4**, 15454-13-4; **5**, 87616-09-9; $EuCl_3$, 10025-76-0.

Contribution from Chemistry Department A,
The Technical University of Denmark, DK-2800 Lyngby, Denmark

Raman Spectroscopic and Spectrophotometric Study of the System $K_2S_2O_7$–$KHSO_4$ in the Temperature Range 200–450 °C

RASMUS FEHRMANN,* NIELS HOLGER HANSEN, and NIELS J. BJERRUM*

Received March 10, 1983

A series of Raman and near-infrared absorption spectra of molten $K_2S_2O_7$–$KHSO_4$ mixtures was obtained at 430 °C in the mole fraction range $X_{K_2S_2O_7}$ = 1.0000–0.1000 and under the equilibrium vapor pressure of water. For molten $KHSO_4$, series of Raman and near-infrared absorption spectra were recorded in the temperature range 200–450 °C. The spectra could best be explained by the presence of the three species involved in the temperature-sensitive equilibrium $2HSO_4^- \rightleftharpoons S_2O_7^{2-} + H_2O$. The structure of $S_2O_7^{2-}$ in the melts was found to be most probably C_{2v} while HSO_4^- presumably has C_s symmetry. No intermediate compound of the three main species was found. Hydrogen bonding between the species seems, however, to be characteristic of the melts. This accounts also for the previously observed low vapor pressure of water. The infrared spectra of $K_2S_2O_7$ in KBr at 25 °C were measured; the spectra agreed well with results obtained by others.

Introduction

Previously[1] we have examined the complex formation of vanadium(V) in pyrosulfate melts as the first step in our attempts to explore the chemistry of melt systems that are idealized examples of the catalyst used for sulfuric acid production. The present investigation is only concerned with the solvent systems based on molten $K_2S_2O_7$–$KHSO_4$ mixtures. The densities of this molten salt system in the whole composition range have been measured previously.[2] The vapor pressures and the phase diagram have been examined[3] (a eutectic was found at 10 mol % $K_2S_2O_7$ with a melting point of 203.5 °C). There seems to be no intermediate compound formed in the system. The remarkable variation in the published melting point for $K_2S_2O_7$ (213–440 °C)[4,5] indicates that the hygroscopic $K_2S_2O_7$ used is in fact partly hydrolyzed to $KHSO_4$. Therefore many investigations have been made on undefined mixtures of the two components. The Raman spectrum of pure molten $K_2S_2O_7$ has as far as we know not been published before. However, Raman bands observed[6] for molten $KHSO_4$ at 300–700 °C were ascribed to $S_2O_7^{2-}$ having C_2 symmetry. The symmetry of $S_2O_7^{2-}$ in the solid state in $K_2S_2O_7$ was found to be C_{2v} on the basis of X-ray data[7] and Raman and IR measurements.[8] The autodissociation reaction $S_2O_7^{2-} \rightleftharpoons SO_4^{2-} + SO_3$ (or perhaps better as $2S_2O_7^{2-} \rightleftharpoons SO_4^{2-} + S_3O_{10}^{2-}$) is up to ca. 500 °C shifted far to the left[9,10] and therefore need not be taken into consideration in connection with the present investigation.

Molten hydrogen sulfates are in many respects different from most ionic salts presumably due to hydrogen bonding. Viscosity and conductance measurements[11] show a high degree of structuralization of the melt, and there is a great tendency to glass formation[12,13] with preservation of the structure in the melt. The published melting point of $KHSO_4$ varies between 207 and 212 °C. This is a much smaller range than the variation mentioned above for the melting point of $K_2S_2O_7$, indicating that commercial $KHSO_4$ probably has a more uniform composition than commercial $K_2S_2O_7$. A significant problem in working with molten bisulfates is the thermal instability of the melt. Above 300 °C an appreciable amount of water is lost possibly due to the decomposition reaction[6]

$$2HSO_4^- \rightleftharpoons H_2O + S_2O_7^{2-} \quad (1)$$

and above 500 °C SO_3 is lost due to decomposition[6]

$$S_2O_7^{2-} \rightleftharpoons SO_3 + SO_4^{2-} \quad (2)$$

Therefore much previous work performed above 300 °C in open cells is probably affected by decomposition.[14] The decomposition up to 500 °C and loss of water can be prevented by applying a fixed vapor pressure of water above the melt.[13,15] In this way the value for the ionic product $[H_2SO_4][SO_4^{2-}]$ related to the self-dissociation reaction

$$2HSO_4^- \rightleftharpoons H_2SO_4 + SO_4^{2-} \quad (3)$$

in molten $KHSO_4$ at 220 °C and P_{H_2O} = 0.041 atm was estimated[13] to be $10^{-2.5}$ mol^2 kg^{-2}. The Raman spectroscopic investigation[6] mentioned above on molten $KHSO_4$ was interpreted in accordance with eq 1. Raman bands ascribed to HSO_4^- decreased while the bands ascribed to $S_2O_7^{2-}$ increased with increasing temperature in the range 300–500 °C. As far as we know, the absorption spectra of molten $KHSO_4$ in the

(1) Hansen, N. H.; Fehrmann, R.; Bjerrum, N. J. *Inorg. Chem.* **1982**, *21*, 744.
(2) Hansen, N. H.; Bjerrum, N. J. *J. Chem. Eng. Data* **1981**, *26*, 13.
(3) Hagisawa, H.; Takai, T. *Bull. Inst. Phys. Chem. Res. Tokyo* **1937**, *16*, 29.
(4) Wickert, K. *Brennst.-Wärme-Kraft* **1959**, *11*, 110.
(5) Spitsyn, V. I.; Meerov, M. A. *Zh. Obshch. Khim.* **1952**, *22*, 905.
(6) Walrafen, G. E.; Irish, D. E.; Young, T. E. *J. Chem. Phys.* **1962**, *37*, 662.
(7) Lynton, H.; Truter, M. R. *J. Chem. Soc.* **1960**, 5112.
(8) Simon, A.; Wagner, H. *Z. Anorg. Allg. Chem.* **1961**, *311*, 102.
(9) Flood, H.; Førland, T. *Acta Chem. Scand.* **1947**, *1*, 781.
(10) Durand, A.; Picard, G.; Vedel, J. *J. Electroanal. Chem. Interfacial Electrochem.* **1976**, *70*, 55.
(11) Rogers, S. E.; Ubbelohde, A. R. *Trans. Faraday Soc.* **1950**, *46*, 1051.
(12) Duffy, J. A.; Glasser, F. P., Ingram, M. D. *J. Chem. Soc. A* **1968**, 551.
(13) Ben Hadid, A.; Picard, G.; Vedel, J. *J. Electroanal. Chem. Interfacial Electrochem.* **1976**, *74*, 145.
(14) Ingram, M. D.; Duffy, J. A.; Forbes, S. M. *J. Appl. Electrochem.* **1971**, *1*, 53.
(15) Ben Hadid, A.; Picard, G.; Vedel, J. *J. Electroanal. Chem. Interfacial Electrochem.* **1976**, *74*, 157.

0020-1669/83/1322-4009$01.50/0